Isomeric states in ^{253}No

A. Lopez-Martens, K. Hauschild, O. Dorvaux, Ch. Briançon, D. Curien, P. Désesquelles, B. Gall, F. Khalfallah, A. Korichi, Marc Rousseau, et al.

EPJ manuscript No.
(will be inserted by the editor)

Isomeric states in ^{253}No

A. Lopez-Martens[1], K. Hauschild[1], A.V. Yeremin[2], O. Dorvaux[3], A.V. Belozerov[2], Ch. Briançon[1], M.L. Chelnokov[2], V.I. Chepigin[2], D. Curien[3], P. Désesquelles[4,1], B. Gall[3], V.A. Gorshkov[2], M. Guttormsen[5], F. Hanappe[6], A.P. Kabachenko[2], F. Khalfallah[3], A. Korichi[1], A.C. Larsen[5], O.N. Malyshev[2], A. Minkova[7,8], Yu.Ts. Oganessian[2], A.G. Popeko[2], M. Rousseau[3], N. Rowley[3], R.N. Sagaidak[2], S. Sharo[9], A.V. Shutov[2], S. Siem[5], L. Stuttgé[3], A.I. Svirikhin[2], N.U.H. Syed[5], and Ch. Theisen[10]

[1] CSNSM, IN2P3-CNRS,UMR8609, F-91405, France
[2] FLNR, JINR, Dubna, Russia
[3] IPHC-DRS, ULP, IN2P3-CNRS, F-67037 Strasbourg, France
[4] Université Paris-Sud, Orsay, F-91405, France
[5] Department of Physics, Oslo University, 0316 Oslo, Norway
[6] Université Libre de Bruxelles, 1050 Bruxelles, Belgium
[7] Faculty of Physics, University of Sofia, 1164 Sofia, Bulgaria
[8] INRNE, BAS, Bulgaria
[9] Department of Physics, Comenius University, SK-84215, Bratislava, Slovakia
[10] CEA-Saclay, DSM/DAPNIA/SPhN, 91191 Gif-sur-Yvette, France

Received: date / Revised version: date

Abstract. Isomeric states in ^{253}No have been investigated by conversion-electron and γ-ray spectroscopy with the GABRIELA detection system. The 31 μs isomer reported more than 30 years ago is found to decay to the ground state of ^{253}No by the emission of a 167 keV M2 transition. The spin and parity of this low-lying isomeric state are established to be $5/2^+$. The presence of another longer-lived isomeric state is also discussed.

PACS. 21.10-k Properties of nuclei – 21.10.Tg Lifetimes – 23.20.Lv gamma transitions and level energies – 23.20.Nx Internal conversion and extranuclear effects

1 Introduction

Isomeric states, i.e. states with strongly inhibited electromagnetic decay modes, occur when there is a secondary energy minimum for some values of shape elongation (shape isomers), total angular momentum of the nucleus (spin isomers) or for a certain value of the projection K of the total angular momentum of the nucleus onto the symmetry axis (K-isomers). Trapped in this pocket, it is difficult for the nucleus to change its shape, spin or its spin orientation relative to the axis of symmetry. In the transfermium region, one expects the occurence of spin-isomers because of the coexistence of high and low-j orbitals close to the Fermi surface [1–6]. K-isomers are also expected because of the combination of nuclear deformation and the presence of orbitals with large spin projections Ω on the symmetry axis. Isomeric states are therefore extremely revealing of the underlying structure of the nucleus: nature and ordering of single-particle states, deformation, configuration of quasiparticle states and magnitude of pairing and/or collective correlations.

K-isomers have been identified in several transfermium nuclei. The gamma-decay of a 70 ns $K^\pi=7^-$ isomeric state was observed by Hall *et al.* in ^{256}Fm [7]. The 1425 keV level, populated in the beta-decay of ^{256m}Es, was also seen to fission with a half-life of 0.8 ms. A 0.28-second isomeric state in ^{254}No and a 1.8-second isomeric state in ^{250}Fm were reported by Ghiorso *et al.* [8] but their quantum numbers could not be determined. By analogy to the interpretation of isomeric states in the A=170-190 around the Hf isotopes, both isomeric states were interepreted as high-spin states, based on either two-proton or two-neutron configurations. It is only very recently, however, that the isomeric state in ^{254}No has been firmly identified as a two-proton $K=8^-$ isomer via the properties of its electromagnetic decay [9,10].

Long-lived spin isomers have been observed in ^{257}Rf [11], ^{253}Lr and ^{257}Db [12], ^{251}No [13] and ^{255}Lr [14]. The isomers in ^{251}No, ^{253}Lr and ^{257}Db involve a low-spin single-particle neutron (for No) or proton (for Lr and Db) state above a high-spin ground state. In ^{257}Rf and ^{255}Lr, the situation is reversed with a high-spin isomeric state above a low-spin ground state. On top of pinning down the sequence of single-particles states, the identification of isomeric states, especially the ones which alpha-decay, is important for the interpretation of the fine structure of alpha-decay. Indeed, the non identification of an isomeric state in a nucleus may lead to the misinterpretation of its quan-

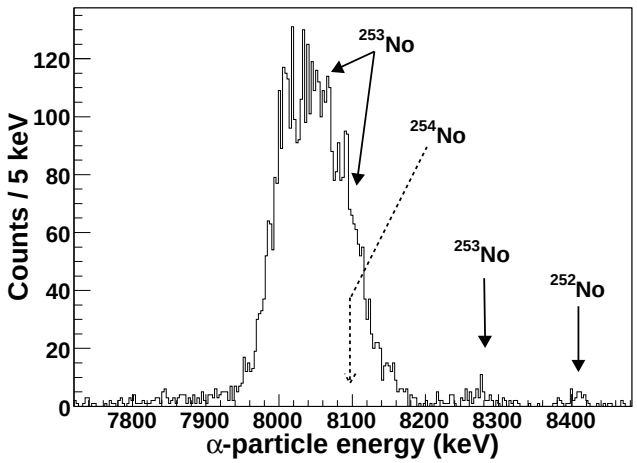

Fig. 1. Energy spectrum of recoil-position-correlated alpha-particles.

tum structure and that of its daughter nucleus. As an example, the reinvistigation of ^{257}Rf revealed the presence of a $11/2^-$ isomeric state, which was responsible for the unusual alpha-decay pattern of ^{257}Rf compared to lighter isotones. This observation modified the spin and parity assignment of the ground state of ^{257}Rf and considerably changed the excitation energy of levels in the daughter nucleus, ^{253}No [11]. In particular, it established the excitation energy of the isomeric state reported by Bemis *et al.* [15] to be 124 keV above the ground state. This energy, however, is lower than the atomic K-binding energy in Nobelium and is incompatible with the delayed X-ray emission observed by Bemis. In this paper, we clarify the situation concerning the low-lying isomeric state in ^{253}No and report on the possible presence of a longer-lived isomeric state.

2 Experimental details

2.1 Experimental set-up

Excited states in ^{253}No were populated in the reaction ^{207}Pb(^{48}Ca,2n) using 350 μg/cm^2 rotating PbS targets on 1.5 μm-thick Ti support foils. The 242 MeV, 0.7 pμA ^{48}Ca beam was provided by the U400 cyclotron of the FLNR, JINR, Dubna. A 2 μm-thick Ti degrader-foil was installed in front of the target in order to have a beam energy of ∼217 MeV at the center of the target. The fusion-evaporation residues (mainly ^{253}No) were transported by the VASSILISSA separator [16,17] and implanted into the stop detector of the GABRIELA detection system [18] installed at the focal plane of the separator. Only nuclear states of the evaporation residues with lifetimes of the order of or larger than the time of flight through the separator (∼ 1μs) will be observed to decay at the focal plane. Evaporation residues are distinguished from the background of scattered beam particles and transfer products by a combined energy and time-of-flight measurement. The background of low-energy scattered particles detected in the stop detector is reduced by placing a mylar foil between the time-of-flight detector and the stop detector. This foil also serves another purpose: it slows down the evaporation residues to reduce their implantation depth in the stop detector. This increases the escape probability of conversion electrons emitted in the backward direction by the implanted nuclei and their daughter products. The conversion electrons are detected in four 4-fold segmented silicon detectors placed upstream from the implantation detector in a tunnel-like configuration. Gamma-ray emission is detected in seven germanium detectors from the French-UK Loan Pool. The signals from each detector are processed individually and time-stamped to a resolution of 1μs. The γ-ray efficiency reaches ∼9% at 120 keV and the electron-detection efficiency peaks at ∼17% for electron energies between 100 and 400 keV.

During the 144-hour experiment, 13000 evaporation residues were identified on the basis of their energy and time-of-flight. This corresponds roughly to half the total number of evaporation residues, which actually reach the stop detector. By requiring an anti-coincidence between the stop detector and the time-of-flight detector, a total of 10500 alpha-decays of $^{252-254}$No were recorded. Using a search time of 10 minutes, 4800 alpha-particles were spatially correlated to recoil events in the stop detector (see Fig. 1). Finally, ∼2 10^6 electrons with energies below 200 keV were detected in the tunnel detectors.

2.2 Lifetime measurement method

The decay properties of a nuclear state can be characterised by the decay probability per unit time λ. If N_r is the number of nuclei produced in such a nuclear state, then the number of decay events per unit time is given by:

$$\frac{dN(t)}{dt} = N_r \lambda e^{(-\lambda t)}. \quad (1)$$

In order to measure the lifetime $\tau = 1/\lambda$ or half-life $T_{1/2} = \ln(2)\tau$ of the state, decay times are generally sorted into a spectrum with time intervals of constant width Δt. In this way, channel i contains the number of decay events observed between t_i and $t_i + \Delta t$. Another way to proceed is to sort decay times into a spectrum with time intervals Δt proportional to time (logarithmic time bins) [19]:

$$\frac{\Delta t}{t} = \text{constant}. \quad (2)$$

By using a change of variables $\theta = \log_2(t) = \ln(t)/\ln(2)$, the density distribution of decays per time bin is given by:

$$\frac{dN(\theta)}{d\theta} = N_r \ln(2)\lambda \times 2^\theta \times e^{\left(-\lambda 2^\theta\right)} \quad (3)$$

This form has the advantage of peaking at θ_{max} which is related to the lifetime of the state by the simple relation

$$\tau = 2^{\theta_{max}} \quad (4)$$

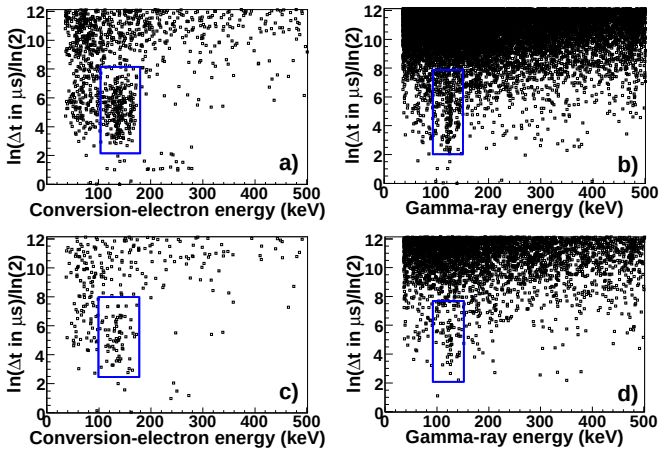

Fig. 2. Energy spectra of conversion electrons (a and c) and gamma-rays (b and d) as a function of $\ln(\Delta t)/\ln(2)$, where Δt is the time difference between the detection of recoils and electrons or gamma-rays. The top panels show the case where all the identified recoils are considered. The bottom panels represent the time differences only for the recoils, which are followed within 10 minutes by the detection of a $^{253-254}$No alpha-particle at the same position in the stop detector. The boxes show the delayed electron and gamma-ray structures mentionned in the text. At large time differences, the spectra are dominated by random correlations.

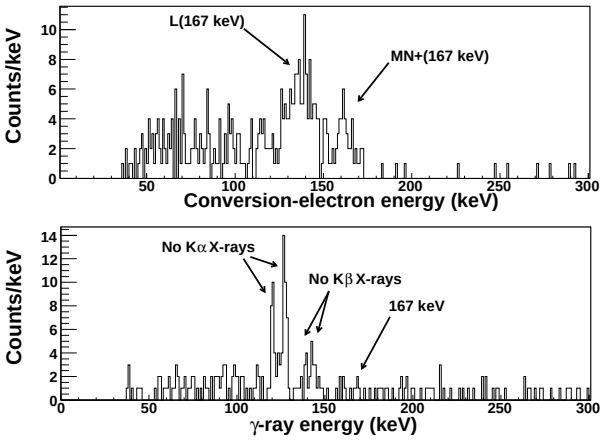

Fig. 3. Energy spectra of conversion electrons (top panel) and γ-rays (bottome panel) emitted 8-128 μs after the detection of a recoil.

It also enables an easy inspection of decay times over a very large interval in time and is particularly well adapted to determine lifetimes in the case of low statistics.

Figure 2 shows the energy spectra of electrons detected in the backward silicon detectors as a function of $\log_2(\Delta t)$, where Δt is the time difference between the detection of any recoil (panel a) or of a $^{253-254}$No-alpha-position-correlated recoil (panel c) in the stop detector and the detection of an electron in the tunnel detectors. In both panels, the same delayed cluster of electrons is clearly visible at electron energies between 120 and 170 keV. A delayed structure around gamma-ray energy 120 keV is visible at similar time differences in panels b and d of Fig. 2. Even though the energy of the ^{254}No alpha-decay coincides with the energy range of the ^{253}No alpha-particle group, the delayed electron and gamma-ray emission seen in Fig. 2 is attributed to ^{253}No since in a dedicated run with a ^{208}Pb target, no such emission was observed in ^{254}No. From equation 4, one can estimate the lifetime of the emitting state to be of the order of $\tau = 2^5 - 2^6$ μs.

In order to measure the lifetime of the above-mentioned isomeric state, equation (1), and therefore also (3), need to be modified to take into account random recoil-electron (or recoil-gamma) correlations [20].

The number $dN(t)$ of electrons detected between times t and $t+dt$ following the implantation of a Nobelium recoil is given by the sum of two independent terms $dN_1(t)$ and $dN_2(t)$. The first term is the number of real decays multiplied by the probability that no other recoil is detected at the focal plane between $t = 0$ and t (i.e., the probability that the next recoil is detected after time t):

$$\frac{dN_1(t)}{dt} = N_r\lambda e^{(-\lambda t)} \int_t^\infty \sigma e^{(-\sigma t)} dt = N_r\lambda e^{(-(\lambda+\sigma)t)} \quad (5)$$

where σ is the recoil rate at the focal plane of VASSILISSA. The integral of this equation over the duration of the experiment yields the number of properly correlated electrons, $N_{tot,1}$. As the duration of the experiment is large compared to the sum of the time constants, $N_{tot,1} = \frac{N_r\lambda}{\lambda+\sigma}$. Conversely, the number of randomly-correlated electrons is given by $N_{tot,2} = N_e - N_{tot,1}$, where N_e is the total number of electrons detected in the experiment.

The second term $dN_2\,(t)$ is the number of random electron events detected in the tunnel multiplied by the probability that no other recoil arrives between $t = 0$ and t. Since the number of random electron events per unit time is given by the product of the number of randomly-correlated electrons $N_{tot,2}$ and of the recoil rate σ:

$$\begin{aligned} \frac{dN_2(t)}{dt} &= N_{tot,2}\sigma \int_t^\infty \sigma e^{(-\sigma t)} dt \\ &= \left(N_e - \frac{N_r\lambda}{\lambda+\sigma}\right) \sigma e^{(-\sigma t)} \end{aligned} \quad (6)$$

Equation (3) therefore becomes:

$$\begin{aligned} \frac{dN(\theta)}{d\theta} &= N_r \ln(2)\lambda 2^\theta e^{\left(-(\lambda+\sigma)2^\theta\right)} \\ &+ \left(N_e - \frac{N_r\lambda}{\lambda+\sigma}\right) \ln(2)\sigma 2^\theta e^{(-\sigma 2^\theta)} \end{aligned} \quad (7)$$

from which the lifetime of the isomeric state can be determined.

2.3 Electromagnetic properties

In Fig. 3 are displayed energy projections (taken between time bins 3 and 7, i.e. between 8 and 128 μs) of the matrices in the top panels of Fig. 2. The K_α and K_β Nobelium X-rays are clearly visible in the spectrum of γ-rays of Fig. 3. In the electron spectrum, two well-separated structures

Table 1. First row: Intensity of the 167 keV γ-ray line as determined experimentally and as determined from the product of the measured X-ray intensity and of the theoretical K-conversion coefficients taken from [22,23]. Second and third rows: Experimental and theoretical ratios of electron-conversion coefficients for the 167 keV transition.

	experiment	E1	E2	E3	M1	M2
I_γ(167 keV)	5(3)	776	820	1035	9	3
α_K/α_{LMN+}	1.3(2)	2.8	0.04	0.002	3.3	1.27
α_L/α_{MN+}	2.8(5)	3.0	2.6	2.4	3.0	2.67

appear at 138 and 161 keV. The nearly flat distribution of counts at lower electron energies corresponds to electrons which backscatter out of the tunnel detectors (see Fig. 4 of reference [18]).

The fact that K X-rays are emitted signifies that a transition of energy greater than the binding energy of K-electrons in Nobelium (150.5 keV) is converted. Furthermore, the energy difference of the two visible electron structures (23(3) keV) corresponds to the average difference in binding energies between the L and M shells in Nobelium ($\sim$20.4 keV). The two electron structures observed in the top panel of Fig. 3 are therefore assigned to the L and $MN+$ conversion of a 167(3) keV transition, which is highly converted. In the γ-ray spectrum of Fig. 3, there are 5(3) counts at 167 keV. In the Nobelium region, the fluorescence yield for a vacancy in the K shell is practically 1 [21]. This means that the observed X-ray intensity can be used as the experimental value for the K-conversion intensity. In Table 1, the expected intensity of the 167 keV γ-ray is reported as a function of the multipolarity and the electromagnetic nature of the 167 keV transition. The ratios of the experimental conversion coefficients are also shown in Table 1 together with the corresponding theoretical values [22,23]. Given all the experimental observations, the 167 keV transition is firmly established to be an M2 transition.

2.4 Lifetime properties

The time projection of the matrix of the top panel of Fig. 2 taken between electron energies 40 and 200 keV, is displayed in Fig. 4. In the bottom panel of Fig. 4, the same electron decay curve is shown using standard constant time bins. When only one decaying state is taken into account, the fit to the electron count distribution (according to equation 7) fails to account for all the intensity. In fact, in the top panel of Fig. 4, the presence of a second isomeric state appears clearly as a second bump around $\ln(\Delta T)/\ln(2)$=10.

If a second isomeric state is included into the parameters of the fit, the lifetime of the isomeric state which decays by the emission of the 167 keV M2 transition, is found to be τ=44.9(3.1) μs. This corresponds to a half-life of $T_{1/2}$=31.1(2.1) μs, which is in agreement with the value given by Bemis *et al.* [15]. The other electron-emitting state has a lifetime of τ=1.4(3) ms ($T_{1/2}$=970(200) μs).

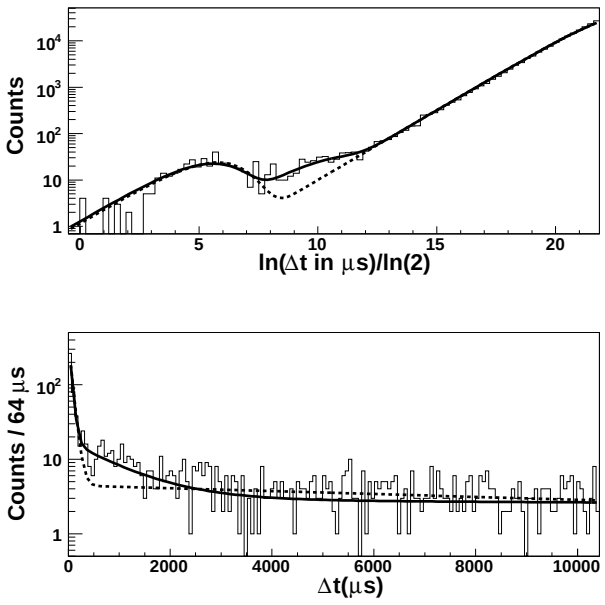

Fig. 4. Distribution of time differences in logaritmic scale (top panel in counts per quarter bins) and linear scale (bottom panel) between the detection of recoils and electrons. The fits to these time distributions are shown for the cases where only the decay of one isomeric state is considered (dashed curves) and when the decay of a second isomeric states is taken into account (solid line).

A consistency check of the fit parameters can be made by comparing the values of (i) the number of recoils, N_r, produced in the short-lived isomeric state, (ii) the total recoil rate, σ, and (iii) the total number of electrons, N_e, detected in the experiment, obtained from the parameters of the fit and the same values obtained by other means. In the case of the shorter-lived isomer, the electron decay curve corresponding to electron energies greater than 120 keV was used to extract a value of N_r = 190(15). In order to find the total number of recoils which were produced in the isomeric state during the experiment, N_r needs to be corrected for the electron-detection efficiency and for the fraction of the intensity of the 167 keV transition which is $LMN+$-converted. This yields N_r = 2513(200). This is well in accordance with the value of N_r which can be extracted from the electron spectrum of Fig. 3. From the intensity of the $LMN+$ structure, the population of the isomeric state is found to be 2100(140). The total recoil rate obtained from the parameters of the fit is σ=2.8(1) $10^{-8}\mu s^{-1}$. This value also fits well with the total number of Nobelium recoils (mainly ^{253}No, but also ^{254}No and ^{252}No) identified during the experiment divided by the duration of the experiment: 2.5 $10^{-8}\mu s^{-1}$. Finally, the total number of electrons detected during the experiment is extracted to be N_e=1.7(1) 10^6. This is in agreement with the 2 10^6 electrons actually detected in the tunnel with energies above the threshold and below 200 keV.

3 Discussion

The ground state of ^{253}No is known to be a $9/2^-$ state [13, 24,25] so the observed excited state which decays to the ground state via an M2 transition must be either a $5/2^+$ or a $13/2^+$ state. The only possible neutron configuration for such a low-lying excited state is the $5/2^+[622]$ neutron hole state (see Fig. 6). This fits well into the systematics of the N=151 isotones [26–29], for which the first excited state can only decay to the ground state via an M2 transition and is therefore isomeric (see figure 5). The energy of the $5/2^+$ state is established to be 167 keV and not 296 keV as it currently tabulated in the Table of Isotopes [30] or 124 keV as is reported in reference [11]. The low energy of this isomeric state in the N=151 isotones is attributed to coupling with a low-lying octupole phonon state. In this experiment, the B(E3) rate and consequently, the degree of collectiviy of the $5/2^+$ state, could not be determined as it has been done for the lighter isotones ^{247}Cm [26] and ^{249}Cf [27]. This is because the uncertainties associated with the conversion coefficients are too large to determine a meaningful M2-E3 mixing ratio.

From the ratio of the number of recoils produced in the short-lived isomeric state of ^{253}No and of the total number of recoils, the population of the 31 μs isomeric state in the fusion-evaporation reaction is estimated to be at least 16(1)%. The rotational band built on the $5/2^+$ state must therefore be populated with similar intensity. This information cannot be ignored in the interpretation of the prompt γ-ray spectra obtained with the multidetectors Gammasphere [29] and Jurogam [31,32] as well as the prompt conversion-electron spectrum obtained with the electron detector Sacred [24,32,33]. This is because the M1 transitions between members of the rotational band built on the $5/2^+$ state will dominate over the cross-over E2 transitions and will contribute to the observed X-ray, low-energy photon and conversion-electron intensities.

The longer-lived isomeric state is assigned to ^{253}No because its lifetime does not coincide with any of the lifetimes of the isomers observed in ^{254}No [9,10], and because the number of nuclei populated in such a state is larger than the number of observed ^{252}No recoils. The energy spectrum of the delayed electron emission is concentrated below 150 keV. The half-life of the state is measured to be 970(200) μs. Given the electron-background conditions and recoil rate, such a half-life is at the limit of the sensitivity of the current experimental setup. Indeed, the energy thresholds of the stop detector prevent the detection of any delayed electron emission below 500-1000 keV at the position of the implanted recoil. A clean and efficient tag on isomeric decays [34] is therefore not available. This is why, given the rather long lifetime of the longer-lived isomeric state and the low efficiency to detect electron-γ-ray coincidences, no γ-ray spectrum with reasonable statistics could be extracted from the background of random recoil-γ-ray correlations.

Although we cannot study the details of the decay of the longer-lived isomeric state, we can exclude and suggest possible configurations based on the available single-particle states shown in Fig. 6. The isomeric state cannot

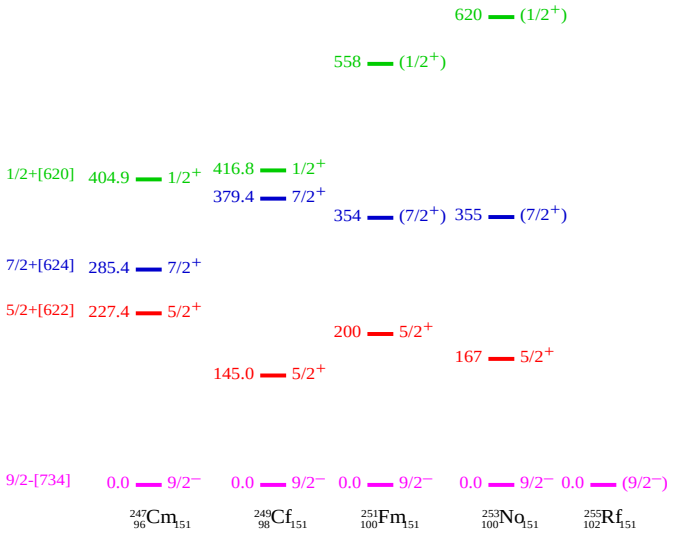

Fig. 5. Systematics of low-lying levels in N=151 isotones obtained from references [26–29] and this work.

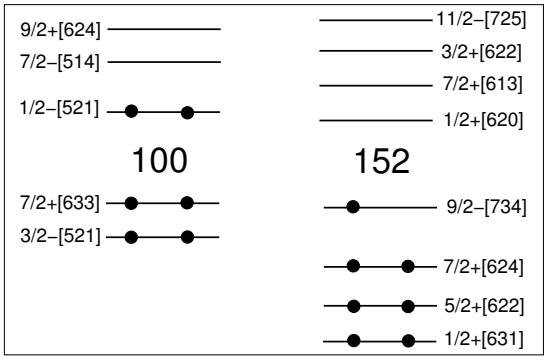

Fig. 6. Schematic representation of the available proton (left) and neutron (right) single-particle levels caclulated in reference [1]. The filled circles illustrate the filling of the orbitals in the ground state of ^{253}No.

be a spin isomer based on the $1/2^+[631]$ or $11/2^-[725]$ single-particle neutron levels, as it is the case in ^{251}No and ^{257}Rf, since it would readily decay to the $5/2^+$ state and ground state respectively. The same reasoning excludes the $1/2^+[620]$ and $3/2^+[622]$ neutron configurations. The isomer is therefore most likely a high-K isomer. In the neighbouring ^{254}No, the $K = 8^-$ isomeric state is based on the $\{9/2^+[624]\pi \otimes 7/2^-[514]\pi\}$ configuration [9,10]. A possible configuration for the isomeric state could therefore be the $\{9/2^+[624]\pi \otimes 7/2^-[514]\pi \otimes 9/2^-[734]\nu\}$ structure with $K^\pi = 25/2^+$. If only neutron excitations are involved, the isomeric state could be based on the $\{9/2^-[734]\nu \otimes 7/2^+[624]\nu \otimes 7/2^+[613]\nu\}$ or $\{9/2^-[734]\nu \otimes 5/2^+[622]\nu \otimes 7/2^+[613]\nu\}$ configurations with $K^\pi = 23/2^-$ and $K^\pi = 21/2^-$ respectively.

To conclude, the isomeric state first observed by Bemis et al. [15] has been shown to decay via an M2 transiton of 167 keV. The state is assigned the $5/2^+[522]$ Nilsson configuration. Its half-life is 31.1(2.1) μs and its popula-

tion in the ^{207}Pb(^{48}Ca,2n) reaction at mid-target beam energies of ∼217 MeV is estimated to be greater than 16%. There is evidence for another, longer-lived isomeric state in ^{253}No, but no spectroscopic information concerning the decay properties of this state could be obtained. To achieve this, tagging on the isomeric decay in the implantation detector is necessary.

The GABRIELA project is jointly funded by JINR (Russia) and IN2P3/CNRS (France). Work at FLNR was performed partially under the financial support of the Russian Foundation for Basic Research, contract N 05-02-16198 and JINR - BMBF (Germany), JINR - Polish, JINR - Slovak Cooperation Programmes. Financial support from the Norwegian Research Council and from the Bulgarian National Foundation, contract N MON-204/06, is also acknowledged.

References

1. R.R. Chasman, I. Ahmad, A.M. Friedman and J.R. Erskine, Rev. Mod. Phys. **49** (1977) 833
2. S. Cwiok, S. Hofmann and W. Nazarewicz, Nucl. Phys. **A 573** (1994) 356
3. A. Parkhomenko and A. Sobiczewski, Acta Phys. Pol. B **35** (2004) 2447
4. A. Parkhomenko and A. Sobiczewski, Acta Phys. Pol. B **36** (2005) 3115
5. M. Bender, P. Bonche, T. Duguet and P.-H. Heenen, Nucl. Phys. **A 723** (2003) 354
6. A.V. Afanasjev, T.L. Khoo, S. Frauendorf, G.A. Lalazissis and I. Ahmad, Phys. Rev **C 67** (2003) 024309
7. H.L. Hall *et al.,* Phys. Rev. **C 39** (1989) 1866
8. A. Ghiorso *et al.,* Phys. Rev. **C 7** (1973) 2032
9. S. K. Tandel *et al.,* Phys. Rev. Lett. **97** (2006) 082502
10. R.-D. Herzberg *et al.,* Nature **442** (2006) 896
11. F.P. Hessberger *et al.,* Z. Phys. **A 359** (1997) 415
12. F.P. Hessberger *et al.,* Eur. Phys. J. **A 12** (2001) 57
13. F.P. Hessberger *et al.,*, Eur. Phys. J **A 22** (2004) 417
14. A. Chatillon *et al.,* Eur. Phys. J **A 30** (2006) 397
15. C.E. Bemis *et al.,* Phys. Rev. Lett. **31** (1973) 647
16. O.N. Malyshev *et. al.,* Nucl. Instr. and Meth. **A440** (2000) 86
17. O.N. Malyshev *et. al.,* Nucl. Instr. and Meth. **A516** (2004) 529
18. K. Hauschild *et al.,* Nucl. Instr. and Meth. **A 560** (2006) 388
19. K.H. Schmidt, Eur. Phys. J. **A 8** (2000) 141
20. M. Leino, S. Yashita and A. Ghiorso, Phys. Rev. **C 24** (1981) 2370
21. M.O. Krause, J. Phys. Chem. Ref. Data **8** (1979) 307
22. R.S. Hager and C. Seltzer, Nucl. Data **A4** (1968) 1
23. O. Dragoun, H.C. Pauli and F. Schmutzler, Nucl. Data **A6** (1969) 235
24. R.-D. Herzberg *et al.,* J. Phys. **G 30** (2004) R123
25. A. Lopez-Martens *et al.,* Phys. Rev. **C 74** (2006) 044303
26. I. Ahmad *et al.,* Phys. Rev. **C 68** (2003) 044306
27. S.W. Yates, R.R. Chasman, A.M. Friedman, I. Ahmad and K. Katori, Phys. Rev. **12** (1975) 442
28. F.P. Hessberger *et al.,* Eur. Phys. J. **A 29** (2006) 165
29. P. Reiter *et al.,* Phys. Rev. Lett. **95** (2005) 032501
30. R.B. Firestone, V.S. Shirley, C.M. Baglin, S.Y.F. Chu and J. Zipkin, Table of Isotopes (John Wiley & Sons, Inc., 8^{th} edition, 1996)
31. P. Greenlees *et al.,* Fusion 06, AIP Proceedings, **Vol. 853** (2006) 416
32. S. Eeckhaudt, PhD thesis, Univeristy of Jyväskylä, Finland (2006)
33. R.-D. Herzberg *et al.,* Eur. Phys. J. **A 15** (2002) 205
34. G.D. Jones, Nucl. Instr. and Meth. **A 488** (2002) 471